

**Beating of the oscillations in the transport coefficients of a
one-dimensionally periodically modulated two-dimensional
electron gas in the presence of spin-orbit interaction**

X. F. Wang* and P. Vasilopoulos[†]

*Department of Physics, Concordia University
1455 de Maisonneuve Ouest, Montréal, Québec, Canada, H3G 1M8*

F.M. Peeters[‡]

*Departement Fysica, Universiteit Antwerpen
(Campus Drie Eiken) Universiteitsplein 1, B-2610 Antwerpen, Belgium*

(Dated: November 9, 2018)

Abstract

Transport properties of a two-dimensional electron gas (2DEG) are studied in the presence of a perpendicular magnetic field B , of a *weak* one-dimensional (1D) periodic potential modulation, and of the spin-orbit interaction (SOI) described only by the Rashba term. In the absence of the modulation the SOI mixes the spin-up and spin-down states of neighboring Landau levels into two new, unequally spaced energy branches. The levels of these branches broaden into bands in the presence of the modulation and their bandwidths oscillate with the field B . Evaluated at the Fermi energy, the n -th level bandwidth of each series has a minimum or vanishes at different values of the field B . In contrast with the 1D-modulated 2DEG without SOI, for which only one flat-band condition applies, here there are two flat-band conditions that can change considerably as a function of the SOI strength α and accordingly influence the transport coefficients of the 2DEG. The phase and amplitude of the Weiss and Shubnikov-de Haas (SdH) oscillations depend on the strength α . For small values of α both oscillations show beating patterns. Those of the former are due to the independently oscillating bandwidths whereas those of the latter are due to modifications of the density of states, exhibit an even-odd filling factor transition, and are nearly independent of the modulation strength. For strong values of α the SdH oscillations are split in two.

PACS numbers: 73.43.Qt 73.61.-r 73.20.-r 85.75.-d

*Electronic address: xuefeng@alcor.concordia.ca

†Electronic address: takis@alcor.concordia.ca

‡Electronic address: peeters@uia.ac.be

I. INTRODUCTION

The magnetotransport of the 2DEG, subjected to periodic potential modulations, has attracted considerable experimental [1] and theoretical [2, 3] attention during the last two decades. For one-dimensional (1D) modulations novel oscillations of the magnetoresistivity tensor $\rho_{\mu\nu}$ have been observed, at low magnetic fields B , distinctly different in period and temperature dependence from the usual Shubnikov-de Haas (SdH) ones observed at higher B . These novel oscillations, referred to as the Weiss oscillations, reflect the commensurability between two length scales: the cyclotron diameter at the Fermi level $2R_c = 2\sqrt{2\pi n_e}\ell_c^2$, with n_e the electron density and ℓ_c the magnetic length, and a the period of the potential modulation.

The emerging field of spintronics brought into the fore the importance of spin-orbit interaction (SOI) in a variety of situations. It is important in the development of spin-based transistors [4], possibly in future quantum computations [5], in an unexpected metal-to-insulator transition in 2D [6] hole gas, in spin-resolved ballistic transport [7], in Aharonov-Casher experiments [8], in spin-galvanic [9] and spin valve [10] effects, in the spin-Hall effect [11], etc. The effect is important in inversely asymmetric bulk semiconductor crystals, due to the internal crystal field, as well in asymmetrically confined semiconductor heterostructures. In the former case the contributions to the spin splitting in the conduction band vary as a $\sim k^3$ term and dominate in *wide-gap* structures [12] whereas in the latter vary as a $\sim k$ term, referred to as the Rashba term, and dominate in *narrow-gap* structures [13]. The latter was confirmed by experiments that showed a zero-magnetic-field spin splitting for carriers with finite momentum in a modulation-doped GaAs/AlGaAs heterojunction [14] as well as by magnetotransport measurements in a 2D hole system [15]. The explanation proposed by Bychkov and Rashba [16] employed the Rashba spin-orbit Hamiltonian, in which the spin of finite-momentum electrons feels a magnetic field perpendicular to the electron momentum in the inversion plane. A detailed account of magnetotransport of the 2DEG in the presence of SOI but absence of modulations appeared recently [17].

Given the importance the SOI has acquired, one question that arises concerns its influence on magnetotransport properties of a 2DEG in the presence of periodic potential modulations. So far we are aware of only the brief, *classical* study of Ref. [18]. Since some effects of the modulations can be explained only quantum mechanically [3], it is of interest to

reexamine the problem *quantum mechanically*. This is the subject of this paper. We will consider only weak 1D modulations and make use of our experience with them [3] and with the unmodulated 2DEG in the presence of SOI [17]. The main qualitative findings are as follows. The levels of the + and -, unequally spaced energy branches, due to the SOI when the modulation is absent, broaden into bands when the modulation is present and their bandwidths oscillate with the field B . Evaluated at the Fermi energy, these bandwidths vanish at different values of the field B and modify considerably the flat-band condition and the transport coefficients as a function of the SOI strength α . As a result, the phase and amplitude of the commensurability and SdH oscillations change when α is varied. For small values of α the former show a beating pattern while for strong values of α the latter are split in two.

In the next section we present the one-electron eigenfunctions and eigenvalues. Analytical results for the conductivities are given in Sec. III and numerical results in Sec. IV. The last section contains a summary and concluding remarks.

II. EIGENFUNCTIONS AND EIGENVALUES

A. A 2DEG in the presence of SOI and absence of potential modulation

We consider a 2DEG in the $(x - y)$ plane and a magnetic field along the z direction. In the Landau gauge $\mathbf{A} = (0, Bx, 0)$ the one-electron Hamiltonian including the Rashba term reads

$$H_0 = \frac{(\mathbf{p} + e\mathbf{A})^2}{2m^*} + \frac{\alpha}{\hbar} [\boldsymbol{\sigma} \times (\mathbf{p} + e\mathbf{A})]_z + \frac{1}{2}g\mu_B B\sigma_z, \quad (1)$$

where \mathbf{p} is the momentum operator of the electrons, m^* is the effective electron mass, g the Zeeman factor, μ_B the Bohr magneton, $\boldsymbol{\sigma} = (\sigma_x, \sigma_y, \sigma_z)$ the Pauli spin matrices, and α the strength of the SOI or Rashba parameter.

Using the Landau wave functions without SOI as a basis, we can express the new eigenfunction in the form:

$$\Psi_{k_y}(\mathbf{r}) = e^{ik_y y} \sum_{n=0}^{\infty} \phi_n(x + x_c) \begin{pmatrix} c_n^+ \\ c_n^- \end{pmatrix} / \sqrt{L_y}. \quad (2)$$

Here $\phi_n(x) = e^{-x^2/2l_c^2} H_n(x/l_c) / (\sqrt{\pi} 2^n n! l_c)^{1/2}$ is the harmonic oscillator function, $\omega_c = eB/m^*$ the cyclotron frequency, $l_c = (\hbar/m^*\omega_c)^{1/2}$ the magnetic length, and the cyclotron

orbit is centered at $x_c = l_c^2 k_y$, n the Landau-level index, and $|\sigma\rangle$ the electron spin written as the row vector $\langle\sigma| = (1, 0)$ if it's pointing up and $(0, 1)$ if it's pointing down.

Using these wave functions and Eq. (1) the eigenvalue problem $H_0\Psi = E\Psi$ leads to an infinite system of equations that can be solved exactly after decomposing it into independent systems of one or two equations [17]. The resulting eigenstates are labelled by a new quantum number s for the energy instead of n . For $s = 0$ there is one level, the same as the lowest Landau level without SOI, with energy

$$E_0^+ = E_0 = \hbar\omega_c/2 - g\mu_B B/2 \quad (3)$$

and wave function

$$\Psi_0^+(k_y) = e^{ik_y y} \phi_0(x + x_c) \begin{pmatrix} 0 \\ 1 \end{pmatrix} / \sqrt{L_y}. \quad (4)$$

For $s = 1, 2, 3, \dots$, there are two branches of levels, denoted by $+$ and $-$, with energies

$$E_s^\pm = s\hbar\omega_c \pm [E_0^2 + 2s\alpha^2/l_c^2]^{1/2}. \quad (5)$$

The $+$ branch is described by the wave function

$$\Psi_s^+(k_y) = \frac{e^{ik_y y}}{\sqrt{L_y \mathcal{A}_s}} \begin{pmatrix} \mathcal{D}_s \phi_{s-1}(x + x_c) \\ \phi_s(x + x_c) \end{pmatrix}, \quad (6)$$

and the $-$ one by

$$\Psi_s^-(k_y) = \frac{e^{ik_y y}}{\sqrt{L_y \mathcal{A}_s}} \begin{pmatrix} \phi_{s-1}(x + x_c) \\ -\mathcal{D}_s \phi_s(x + x_c) \end{pmatrix}, \quad (7)$$

where $\mathcal{A}_s = 1 + \mathcal{D}_s^2$ and $\mathcal{D}_s = (\sqrt{2s}\alpha/l_c)/[E_0 + \sqrt{E_0^2 + 2s\alpha^2/l_c^2}]$.

B. A 2DEG in the presence of SOI and of a 1D potential modulation

In the presence of a 1D periodic electric modulation, we consider the Hamiltonian

$$H = H_0 + V_0 \cos(Kx), \quad (8)$$

with $K = 2\pi/a$ and a the modulation period. For weak modulations the energy correction due to the term $V_0 \cos(Kx)$ is evaluated by first-order perturbation theory. The results for the two branches are

$$E_s^\pm = s\hbar\omega_c + [E_0^2 + 2s\alpha^2/l_c^2]^{1/2} + V_0 e^{-u/2} \cos(Kx_c) [\mathcal{D}_s^2 L_{s-1}(u) + L_s(u)] / \mathcal{A}_s; \quad s = 0, 1, \dots \quad (9)$$

$$E_s^- = s\hbar\omega_c - [E_0^2 + 2s\alpha^2/l_c^2]^{1/2} + V_0 e^{-u/2} \cos(Kx_c) [L_{s-1}(u) + \mathcal{D}_s^2 L_s(u)] / \mathcal{A}_s; \quad s = 1, 2, \dots \quad (10)$$

where $u = 2\pi^2 l_c^2 / a^2 = K^2 l_c^2 / 2$ and $x_c = k_y l_c^2$. $L_s(u)$ is the Laguerre polynomial and for $s = 0$ Eq. (9) reduces to Eq. (3) as modified by the perturbation correction. The width of the broadened levels of the two branches is given by twice the absolute value of the last term in Eqs. (9) and (10) without the $\cos(K l_c^2 k_y)$ factor and is denoted by $2|\Delta_s^\pm|$. Δ_s^\pm can be written in the compact form

$$\Delta_s^\pm = V_0 e^{-u/2} [L_{s-1/2 \pm 1/2} + \mathcal{D}_s^2 L_{s-1/2 \mp 1/2}] / \mathcal{A}_s, \quad (11)$$

with the upper signs pertaining to the + branch and the lower ones to the - branch; obviously Δ_s^\pm is not the same for the two branches. In contrast, without SOI we have only a single branch and a single bandwidth [3] and the eigenvalues are given, when the Zeeman term is neglected, by

$$E_n = (n + 1/2)\hbar\omega_c + V_0 e^{-u/2} \cos(Kx_c) L_n(u) \quad (12)$$

with n the Landau-level index. This has consequences that will be detailed below.

As in the absence of SOI, the presence of the modulation broadens the discrete levels into bands. An important difference with the situation in which the modulation is absent is that the diagonal matrix elements of the velocity operator now do not vanish. Using $v_y^\pm = (1/\hbar) \partial E_s^\pm(k_y) / \partial k_y$ their values are

$$v_y^+ = -2V_0 u e^{-u/2} [\mathcal{D}_s^2 L_{s-1}(u) + L_s(u)] \sin(Kx_c) / (\hbar K \mathcal{A}_s), \quad (13)$$

$$v_y^- = -2V_0 u e^{-u/2} [L_{s-1}(u) + \mathcal{D}_s^2 L_s(u)] \sin(Kx_c) / (\hbar K \mathcal{A}_s). \quad (14)$$

These non vanishing values lead to a non vanishing diffusive conductivity whereas in the absence of the modulation this conductivity vanishes whether the SOI is present or not [17]. Compared to the case without SOI, we have two contributions, one from Eq. (9) and one from Eq. (10), while for $\alpha = 0$ we have only one value given by

$$v_y = -(2V_0 / \hbar K) u e^{-u/2} L_n(u) \sin(Kx_c). \quad (15)$$

As a function of the magnetic field B , these v_y^\pm contributions do not oscillate in phase due to the different dependence of the Laguerre polynomials on B . This modifies mostly the diffusive conductivity in the presence of the modulation and will be detailed in the following sections.

Using the asymptotic expression of the Laguerre polynomials for large s , we obtain $\Delta_s^\pm \propto \cos(2\sqrt{su} - \pi/4)$. The Landau level indices s^+ and s^- of the corresponding branches at the Fermi energy can be determined by the equations $E_{s^+}^+ \approx E_{s^-}^-$ and $n_e = (s^+ + s^- + 1)/(2\pi l_c^2)$, where n_e is the electron density. Then from the argument of $\cos(2\sqrt{su} - \pi/4)$ we obtain the flat-band conditions

$$\sqrt{u}[\sqrt{\pi n_e} l_c \mp \alpha / (\sqrt{2} \hbar \omega_c l_c)] = \pi(i - 1/4)/2 \quad (16)$$

with the upper (lower) sign corresponding to the $+$ ($-$) branch. Since the cyclotron radius at the Fermi energy is $R_c^\pm = l_c \sqrt{2s^\pm + 1}$, Eq. (16) can be written as $2R_c^\pm/a = i - 1/4$ with $R_c^\pm = R_c^0 \mp \alpha/\hbar\omega_c$ and R_c^0 the cyclotron radius without SOI or $K(k_F \mp k_\alpha)l_c^2 = \pi(i - 1/4)$ with $k_F = \sqrt{2\pi n_e}$, and $k_\alpha = \alpha m^*/\hbar^2$. The same result has been obtained in Ref. [18] by a purely classical treatment. The fact that now we have *two* flat-band conditions, as opposed to *one* for $\alpha = 0$, leads to oscillations with *two* different frequencies and consequently to beating patterns that will be shown in Sec. IV. Explicitly, writing Eq. (16) again for $i \rightarrow i + 1$ and subtracting the result from Eq. (16), gives the periods in the \pm branches as $\Omega^+ = ea/[2\hbar(k_F - k_\alpha)]$ and $\Omega^- = ea/[2\hbar(k_F + k_\alpha)]$.

III. CONDUCTIVITIES

For weak electric fields E_ν , i.e., for linear responses, and weak scattering potentials the expressions for the direct current (dc) conductivity tensor $\sigma_{\mu\nu}$, in the one-electron approximation, reviewed in Ref. [21], reads $\sigma_{\mu\nu} = \sigma_{\mu\nu}^d + \sigma_{\mu\nu}^{nd}$ with $\mu, \nu = x, y, z$. The terms $\sigma_{\mu\nu}^d$ and $\sigma_{\mu\nu}^{nd}$ stem from the diagonal and nondiagonal part of the density operator $\hat{\rho}$, respectively, in a given basis and $\langle J_\mu \rangle = Tr(\hat{\rho} J_\mu) = \sigma_{\mu\nu} E_\nu$. In general, we have $\sigma_{\mu\nu}^d = \sigma_{\mu\nu}^{dif} + \sigma_{\mu\nu}^{col}$. The term $\sigma_{\mu\nu}^{dif}$ describes the diffusive motion of electrons and the term $\sigma_{\mu\nu}^{col}$ the collision contributions or hopping. The former is given by

$$\sigma_{\mu\nu}^{dif} = \frac{\beta e^2}{S_0} \sum_{\zeta} f(E_s^\sigma) [1 - f(E_s^\sigma)] \tau^\zeta (E_s^\sigma) v_\mu^\zeta v_\nu^\zeta, \quad (17)$$

where $\zeta \equiv (s, \sigma, k_y)$ denotes the quantum numbers, $v_\mu^\zeta = \langle \zeta | v_\mu | \zeta \rangle$ is the diagonal element of the velocity operator v_μ , and $f(\varepsilon)$ the Fermi-Dirac function. Further, $\tau^\zeta(E_s^\sigma)$ is the relaxation time for elastic scattering, $\beta = 1/k_B T$, and S_0 is the area of the system.

The term $\sigma_{\mu\nu}^{col}$ can be written in the form

$$\sigma_{yy}^{col} = \frac{\beta e^2}{2S_0} \sum_{\zeta, \zeta'} \int_{-\infty}^{\infty} d\varepsilon \int_{-\infty}^{\infty} d\varepsilon' \delta[\varepsilon - E_s^\sigma(k_x)] \delta[\varepsilon' - E_{s'}^{\sigma'}(k'_x)] f(\varepsilon) [1 - f(\varepsilon')] W_{\zeta\zeta'}(\varepsilon, \varepsilon') (y_\zeta - y_{\zeta'})^2, \quad (18)$$

where $y_\zeta = \langle \zeta | y | \zeta \rangle$; $W_{\zeta\zeta'}(\varepsilon, \varepsilon')$ is the transition rate. For elastic scattering by dilute impurities, of density N_I , we have

$$W_{\zeta\zeta'}(\varepsilon, \varepsilon') = \frac{2\pi N_I}{\hbar S_0} \sum_{\mathbf{q}} |U(\mathbf{q})|^2 |F_{\zeta\zeta'}(u)|^2 \delta(\varepsilon - \varepsilon') \delta_{k_x, k'_x - q_x}, \quad (19)$$

where $u = l_c^2 q^2 / 2$ and $q^2 = q_x^2 + q_y^2$. $U(\mathbf{q}) = (e^2 / 2\epsilon_0 \epsilon) / (q + k_s)$ is the Fourier transform of the screened impurity potential with ϵ the static dielectric constant, ϵ_0 the dielectric permittivity, and k_s the screening wave vector.

The diffusion contribution given by Eq. (17) becomes

$$\sigma_{yy}^{dif} = \frac{e^2}{h} \frac{4\beta u^2 \tau}{\pi K} \sum_{s, \sigma} \int_0^{a/2l_c^2} dk_y (\Delta_s^\sigma)^2 \sin^2(K l_c^2 k_y) f(E_{n, k_y}^\sigma) [1 - f(E_{n, k_y}^\sigma)] \quad (20)$$

with $\Delta_s^\sigma = \Delta_s^\pm$ given by Eq. (11). The related contribution σ_{xx}^{dif} is zero since the velocity v_x vanishes.

For weak potential modulations we can neglect Landau-level mixing, i.e., we can take $s' = s$. Then noting that $\sigma_{xx}^{col} = \sigma_{yy}^{col}$, $\sum_{\mathbf{q}} = (S_0 / 2\pi) \int_0^\infty q dq = (S_0 / 2\pi l_c^2) \int_0^\infty du$, and $\sum_{k_x} = (S_0 / 2\pi l_c^2)$, the collisional contribution given by Eq. (18) takes the form

$$\sigma_{yy}^{col} = \frac{e^2}{h} \frac{N_I \beta}{2A_0} \sum_{s, \sigma, k_y} \int_0^\infty du |F_{ss}^\sigma(u)|^2 u \int_{-\infty}^\infty d\varepsilon [\delta(\varepsilon - E_s^\sigma)]^2 f(\varepsilon) [1 - f(\varepsilon)] |U(\sqrt{2u/l_c^2})|^2, \quad (21)$$

where

$$|F_{ss}^-(u)|^2 = \{L_{s-1}(u) + \mathcal{D}_s^2 L_s(u)\}^2 e^{-u} / \mathcal{A}_s^2, \quad (22)$$

$$|F_{ss}^+(u)|^2 = \{\mathcal{D}_s^2 L_{s-1}(u) + L_s(u)\}^2 e^{-u} / \mathcal{A}_s^2. \quad (23)$$

The exponential e^{-u} favors small values of u . Assuming $b = k_s^2 l_c^2 / 2 \gg u$ we may neglect the term $2u/l_c^2$ in the expression for $U(\sqrt{2u/l_c^2})$ and define $U_0 = U(0)$. We then obtain

$$\sigma_{yy}^{col} = \frac{e^2}{h} \frac{N_I U_0^2 \beta}{\pi a \Gamma} \sum_{s, \sigma} \int_0^{a/2l_c^2} dk_y I_s^\sigma f(\varepsilon) [1 - f(\varepsilon)], \quad (24)$$

where

$$I_s^\pm = [(2s \pm 1)\mathcal{D}_s^4 - 2s\mathcal{D}_s^2 + 2s \pm 1]/\mathcal{A}_s^2. \quad (25)$$

The impurity density N_I determines the Landau Level broadening $\Gamma = W_{\zeta\zeta'}(\varepsilon, \varepsilon')/\hbar$. Evaluating $W_{\zeta\zeta'}(\varepsilon, \varepsilon')/\hbar$ in the $u \rightarrow 0$ limit without taking into account the SOI, we obtain $N_I \approx 4\pi[(2\varepsilon\varepsilon_0/e^2)]^2\Gamma/\hbar$.

The Hall conductivity σ_{xy}^{nd} is given by

$$\sigma_{xy}^{nd} = \frac{2i\hbar e^2}{S_0} \sum_{\zeta, \zeta'} f(E_\zeta)[1 - f(E'_\zeta)] \langle \zeta | v_x | \zeta' \rangle \langle \zeta' | v_y | \zeta \rangle \frac{1 - e^{\beta(E_\zeta - E'_\zeta)}}{(E_\zeta - E'_\zeta)^2}, \quad \zeta' \neq \zeta. \quad (26)$$

The resistivity tensor $\rho_{\mu\nu}$ is given in terms of the conductivity tensor $\sigma_{\mu\nu}$ upon using the standard expressions $\rho_{xx} = \sigma_{yy}/S$, $\rho_{yy} = \sigma_{xx}/S$, $\rho_{yx} = \rho_{xy} = -\sigma_{yx}/S$, where $S = \sigma_{xx}\sigma_{yy} - \sigma_{xy}\sigma_{yx}$.

IV. NUMERICAL RESULTS

In this section we present numerical results for the bandwidth and the two conductivities given by Eqs. (20) and (23) for various values of the SOI strength α , of the modulation strength V_0 and period a , of the electron density n_e , and of the temperature T . We measure α in units of $\alpha_0 = 10^{-11}$ eVm, n_e in units of $n_0 = 10^{-11}/\text{cm}^2$, and use the effective mass of InAs $m^* = 0.05m_0$ with m_0 the free-electron mass.

In Fig. 1 we plot Δ_s^\pm , given by Eq. (11) and directly related to the bandwidth $2|\Delta_s^\pm|$, at the Fermi level, as a function of the magnetic field B in the upper panels and as a function of the inverse magnetic field $1/B$ in the lower panels. The other parameters are $a = 3500 \text{ \AA}$, $T = 2 \text{ K}$, $n_e = 3n_0$, and $V_0 = 0.5 \text{ meV}$. We plot Δ_s^\pm and not $2|\Delta_s^\pm|$ so that the oscillations are seen more clearly. Comparing the $\alpha = 0$ panel with the $\alpha \neq 0$ ones, we see clearly, for $\alpha \neq 0$, the contributions from the + and - branches. The large-amplitude oscillations, for low B in the upper panels and for high $1/B$ in the lower panels, are the Weiss oscillations whereas the step-like behavior on the right side of the upper panels is due to the small-amplitude SdH ones. On the scale used the latter are barely visible on the very left side in the lower panels. The phase shift between the oscillations of Δ_s^+ and Δ_s^- and their slightly different frequencies described by Eq. (16) lead to the beating patterns of the conductivities shown below. For example, for $\alpha = 2\alpha_0$ the oscillations of the bandwidth $2|\Delta_s^\pm|$, given after Eq.

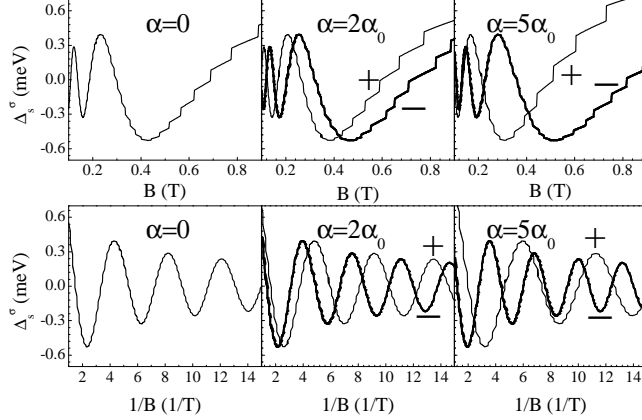


FIG. 1: The quantity Δ_s^\pm of Eq. (11) vs magnetic field B (upper panels) and vs inverse magnetic field $1/B$ (lower panels), at the Fermi level, for different values of the strength α . The modulation period is $a = 3500\text{\AA}$ and the modulation strength $V_0 = 0.5\text{meV}$.

(16), have a period $\Omega^+ = 2.14 \text{ T}^{-1}$ in the + branch and a period $\Omega^- = 1.76 \text{ T}^{-1}$ in the - branch.

In Fig. 2 we plot the conductivities vs the inverse of the magnetic field B for different values of α and a shorter modulation period $a = 800 \text{\AA}$. The upper curve is the collisional conductivity, given by Eq. (23), and the lower one the diffusive conductivity, given by Eq. (20). Notice the absence of a beating pattern for $\alpha = 0$ and its development for $\alpha \neq 0$. For finite α , the longer-period beating pattern of the Weiss oscillations is observed in the diffusive curves and the shorter-period beating pattern of the SdH oscillations [17] in the collisional curves. The reason is that at low magnetic fields and low temperatures the Weiss oscillations dominate the diffusive conductivity while the SdH oscillations dominate the collisional conductivity. In the former the energy correction due to the modulation, given by Eqs. (9)-(10), enters mainly the square of v_y^\pm and the argument of the Fermi function, cf. Eqs. (17), (20), whereas in the latter it enters essentially only through the argument of the Fermi function, cf. Eqs. (18), (24).

To see the oscillations shown in Fig. 2 more clearly, we plot the conductivities vs filling

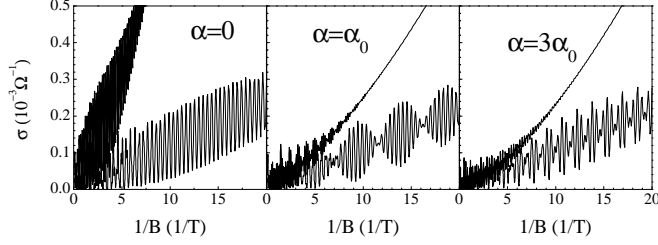


FIG. 2: Conductivities vs inverse magnetic field B for different values of α with $a = 800\text{\AA}$, $T = 1\text{K}$, $n_e = 3n_0$, and $V_0 = 0.3\text{ meV}$. The upper (lower) curves show the collisional (diffusive) contribution.

factor nh/eB in Fig. 3 for $\alpha = \alpha_0$ and $n_e = 3n_0$. As can be seen, the collisional conductivity (upper curve) shows a beating pattern of the SdH oscillations resulting from the different Landau-level separations in the $+$ and $-$ spin branches. The index s^\pm at the Fermi energy is expressed approximately as $s^\pm = (\pi n_e \hbar \mp m^* \alpha \sqrt{2\pi n_e} / \hbar) / eB$. The resulting period of the beating pattern, measured in units of inverse magnetic field, is $2\hbar k_\alpha k_F / e$ or 0.85T^{-1} in Fig. 3. We notice that a transition from conductivity maxima at *even* filling factors to conductivity maxima at *odd* filling factors occurs between adjacent wraps of the SdH oscillations. This can be understood by checking the DOS of the system. As shown in Fig. 4, when the subband broadening is comparable to the subband separation, a beating pattern appears in the DOS, with SOI present and modulation absent, and each DOS peak corresponds to one pair of spin levels. Because the spin-up and spin-down levels have different separations, there is one unpaired spin level at each node of the beating pattern. As a result, in one wrap of the DOS oscillations there is an *even* number of levels below each pair and the DOS has a peak at *odd* filling factors, while in the next wrap there is an *odd* number of levels below each pair and the DOS has a peak at *even* filling factors. When the Fermi energy passes through the \pm branches and the DOS is as described above, the collisional conductivity shows a beating pattern with an *even-odd* filling factor transition. Although here the modulation is present, it is very weak and leaves the oscillations of the collisional conductivity nearly intact. A complementary way of seeing how the beating pattern is formed, is to plot separately $\sigma^{col,-}$ and $\sigma^{col,+}$. Both contributions oscillate with slightly different frequencies and their sum shows the beating pattern of Fig. 3. The period of this pattern, in units of inverse of magnetic field, is $ea/4\hbar k_\alpha$ or 4.63T^{-1} in Fig. 3. A similar even-odd filling factor transition was also observed for *strong* modulations, which make the Landau levels overlap, in the absence of SOI and was explained by the behavior of the corresponding DOS [22]. The

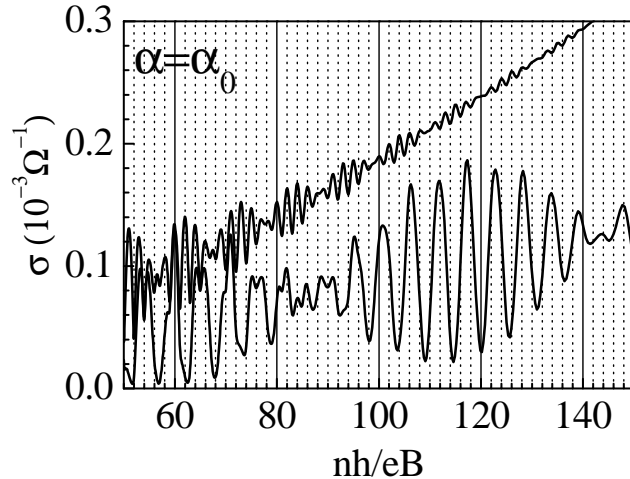


FIG. 3: Conductivities vs filling factor nh/eB for the panel $\alpha = \alpha_0$ of Fig. 2. The dashed vertical lines show the even filling factor values and the curves are marked as in Fig. 2.

diffusive conductivity (lower curve) shows mainly a beating pattern of the Weiss oscillations since here the SdH oscillations are very weak.

Above we observed a beating pattern in the SdH and Weiss oscillations occurring, respectively, in the collisional and diffusive conductivities, vs filling factor when varying the magnetic field at a fixed electron density. If we vary the electron density and fix the magnetic field B , the beating pattern of the SdH oscillations holds because it corresponds to the Fermi energy passing through the DOS with beating pattern. However, we do not observe a beating pattern in the Weiss oscillations. This can be explained by Eq. (16), from where we see that, for fixed B , the bandwidths of the two series of spin levels oscillate with the same frequency as a function of the electron density n_e though with different phases. For a system without the potential modulation, the diffusive conductivity disappears and we observe only a beating pattern of the SdH oscillations in the collisional conductivity.

In Fig. 5 we plot again the conductivities vs the inverse of the magnetic field B for different values of the temperature, $\alpha = \alpha_0$, $n_e = 3n_0$, and $V_0 = 0.3$ meV. The two curves are marked as in Fig. 2. Notice that beating pattern exists for all temperatures but the oscillation amplitude decreases with increasing temperature and nearly disappears at $T \approx 5$ K for the density and SOI strength used.

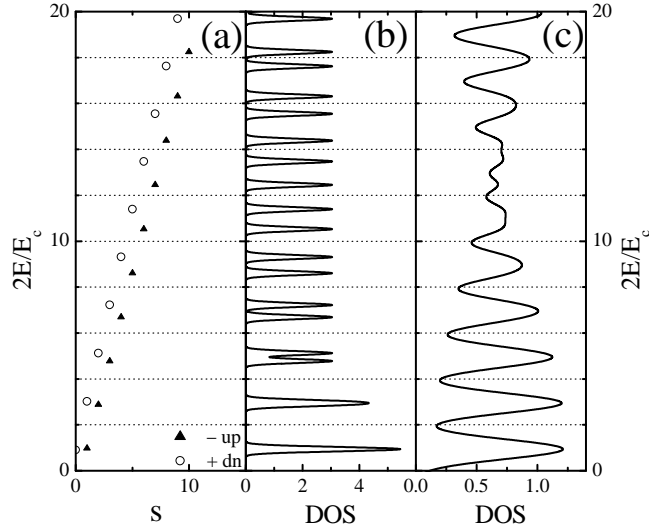


FIG. 4: (a) Subband energy vs index s in the absence of modulation. The DOS vs energy is shown in (b) for subband broadening $\Gamma = 0.1$ meV and in (c) for $\Gamma = 0.5$ meV. When E is the Fermi energy the quantity $2E/E_c$ with $E_c = \hbar\omega_c$ is approximately the filling factor.

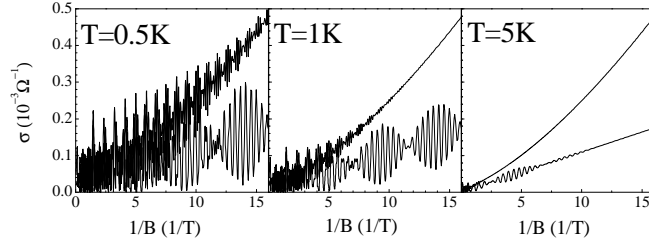


FIG. 5: Conductivities vs inverse magnetic field B for different temperatures with $\alpha = \alpha_0$ and $n_e = 3n_0$. The upper (lower) curves show the collisional (diffusive) contribution.

In Fig. 6 we plot the conductivities vs magnetic field B , for rather strong values of B , and different α . The temperature is $T = 1K$. The dotted (solid) curves show the collisional (diffusive) conductivity. The SOI splits each Landau subband and reduces the DOS inside it. As a result, a reduction in the oscillation amplitude and a splitting of the (SdH) oscillations are observed in the $\alpha = 2\alpha_0$ panel compared with the $\alpha = 0$ one. For the high magnetic fields involved here, the period of the Weiss oscillations is very long and both the diffusive

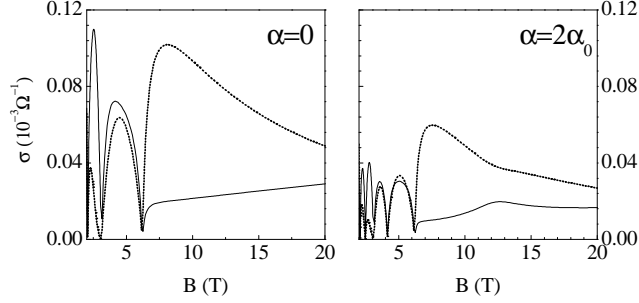


FIG. 6: Conductivities vs magnetic field B for two different values of α . The temperature is $T = 1\text{K}$ and the density $n_e = 3n_0$. The dotted (solid) curves show the collisional (diffusive) conductivity.

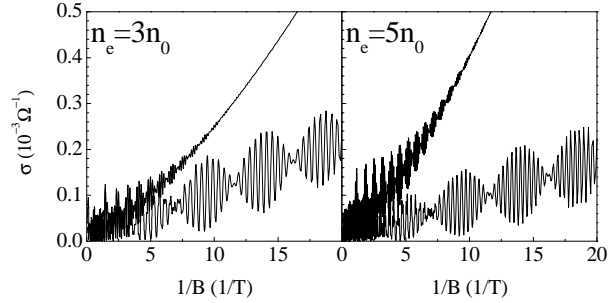


FIG. 7: Conductivities vs inverse magnetic field B for different densities, $\alpha = \alpha_0$, and temperature $T = 1\text{K}$. The upper (lower) curves show the collisional (diffusive) conductivity.

and collisional conductivity curves show the SdH oscillations with the same phase.

In Fig. 7 we plot the conductivities vs magnetic field B for different densities, $\alpha = \alpha_0$, and temperature $T = 1\text{K}$. Again the two curves are marked as in Fig. 2. Notice how increasing the density and thus changing the position of the Fermi level relative to those of the $+$ and $-$ branches closest to it modifies the beating pattern.

In Fig. 8 we plot the conductivities vs magnetic field B for different α . The density is $n_e = 3n_0$ and the temperature $T = 2\text{K}$. The upper (lower) curves are the collisional (diffusive) contributions. The diffusive curve shows mainly the Weiss oscillations at low B and at high B the short-period SdH oscillations in addition to the long-period Weiss oscillations. The collisional curve shows clearly the SdH oscillations for $\alpha = 0$ and a beating

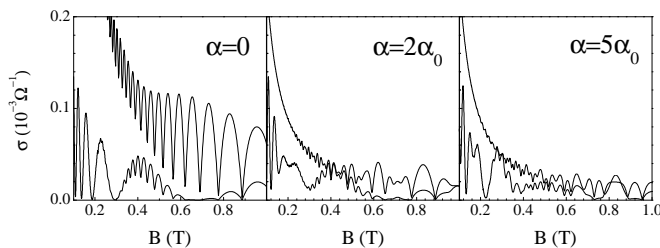


FIG. 8: Conductivities vs magnetic field B for different α . The density is $n_e = 3n_0$, the modulation period $a = 3500\text{\AA}$, and the temperature $T = 2$ K. The upper (lower) curves show the collisional (diffusive) conductivity.

pattern of the SdH oscillation for finite α .

We now address the issue of the Hall conductivity σ_{xy}^{nd} . In the absence of modulation and presence of SOI, it has been evaluated in Ref. [17] for rather *strong* fields $B \geq 1$ T and shows two series of quantum Hall plateaus, for *strong* α ($\alpha \approx 10\alpha_0$), corresponding to the two branches developed due the SOI. The 1D modulation removes the k_y degeneracy of the Landau levels E_s and broadens them into bands with eigenvalues E_{s,k_y} . From Eq. (26) we see that this may affect the Hall conductivity at weak magnetic fields when the broadening Δ_s is comparable to the energy $\hbar\omega_c$. In the presence of modulation and absence of SOI, it has been evaluated in Ref. [3] for *weak* fields $B \leq 1$ T and shows very small-amplitude oscillations expressed mainly through the energy difference between the n and $n \pm 1$ Landau levels. Here the interest is in the region of *weak* fields $B \leq 1$ T for which the Weiss oscillations appear. Despite the fact that Δ_s is comparable to $\hbar\omega_c$, it exhibits again very small-amplitude oscillations so far not observed for *weak* modulations [23]. If we neglect these oscillations, it is approximately given by $\sigma_{xy}^{nd} \approx ne/B$.

Experimentally one usually measures the resistivity $\rho_{\mu\nu}$. Using the expressions given at the end of Sec. III for $\rho_{\mu\nu}$, $\sigma_{xy}^{nd} \approx ne/B$, and the results for σ_{yy} and σ_{xx} , we show in Fig. 8 the resistivities divided by the magnetic field ρ_{xx}/B , for $\alpha = \alpha_0$ (upper panel) and $\alpha = 3\alpha_0$ (lower panel), as a function of the magnetic field for a system with $n_e = 3n_0$ and otherwise the same parameters as in Fig. 7. For $\alpha = \alpha_0$ and in the low-field region, in which the SdH oscillations are absent, a beating pattern of the Weiss oscillations is clearly observed in the ρ_{xx} curve. The ρ_{yy} curve exhibits a beating pattern only for the SdH oscillations since they

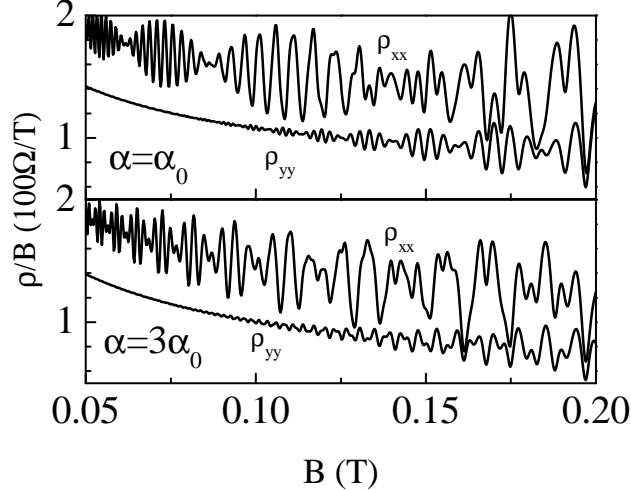


FIG. 9: Resistivities divided by the field B , ρ_{xx}/B and ρ_{yy}/B , vs field B for $\alpha = \alpha_0$ (upper panel) and $\alpha = 3\alpha_0$ (lower panel). The other parameters are the same as in Fig. 2.

result only from collisional current contributions and the Weiss oscillations are very weak as the diffusive contributions to $\rho_{yy} \propto \sigma_{xx}$ vanish. For $\alpha = 3\alpha_0$ though the beating patterns change: that of the Weiss oscillations, when discernible in ρ_{xx} , becomes shorter and that of the SdH oscillations in ρ_{yy} disappears. For completeness it should be mentioned, though not shown, that for $\alpha = 0$ there are no beating patterns in either the Weiss [3] or SdH [17] oscillations.

V. CONCLUDING REMARKS

We evaluated *quantum mechanically* the dc conductivities of a 2DEG in the presence of SOI of strength α , of a normal magnetic field B , and of a *weak* 1D potential modulation of strength V_0 and of period a . The SOI splits the Landau levels, for $\alpha = 0$, in two unequally spaced energy branches. As in the absence of SOI, the modulation broadens the levels of these branches into bands and their bandwidths oscillate independently with the field B . This gives rise to two flat-band conditions, instead of one for $\alpha = 0$, and to the beating patterns of the Weiss oscillations. As for the SdH oscillations, their beating patterns for weak α are nearly independent of the modulation, at least as long as the latter is weak, and agree with those of Ref. 17 obtained in the absence of modulation. However, for strong α an additional structure is obtained and the SdH oscillations split in two, cf. Fig. 6. We

also noticed the even-odd filling factor transition in the SdH oscillations and explained it with the help of the broadened DOS. A similar observation was made in Ref. 22 for strong modulations and was explained by the corresponding DOS.

Regarding the Weiss oscillations the results for the diffusive conductivity agree, as expected, for the relevant weak magnetic fields and high quantum numbers s , with those of the *classical* evaluation of Ref. [18]. However, the results for the collisional conductivity could not be obtained by a *classical* treatment and, to our knowledge, are new. It is well known that this collisional or hopping conductivity describes the SdH oscillations which cannot be treated *classically*. This explains their absence from Ref. [18] and their modification for strong α as well as for strong B , cf. Fig. 6, presented here.

For weak α both conductivities exhibit beating patterns. Those of the diffusive conductivity pertain to the Weiss oscillations and are due to the two independent frequencies involved in the bandwidths of the $+$ and $-$ branches created by the SOI whereas those of the collisional conductivity pertain to the SdH oscillations and have a similar explanation though the two frequencies involved here are not those of the bandwidths, see the discussion of Fig. 3. As we saw though, these patterns weaken or disappear rather quickly upon increasing the temperature or the strength α . On the electron density n_e though, they appear to have a rather weak dependence, cf. Fig. 7, at least as long as n_e falls in the range of the usual experimental densities of a 2DEG.

We are not aware of any directly relevant experimental work. We hope though that the findings described above will motivate experiments in which the magnetoresistivities along the x and y directions could be measured in a weakly modulated 2DEG in the presence of SOI. For a 1D modulation along the x direction, the diffusive and collisional contributions to the conductivity can be obtained separately using the relations $\sigma_{yy} = \sigma_{yy}^{dif} + \sigma_{yy}^{col}$ and $\sigma_{xx} = \sigma_{xx}^{col}$. Combining them with the standard relations given after Eq. (26), gives the magnetoresistivities.

Acknowledgments

This work was supported by the Canadian NSERC Grant No. OGP0121756, by the Flemish Science Foundation (FWO-VI), the Belgian Science Policy, and the EU-CERION

project.

-
- [1] D. Weiss, K. von Klitzing, K. Ploog, and G. Weimann, *Europhys. Lett.* **8**, 179 (1989); R. W. Winkler, J.P. Kotthaus, and K. Ploog, *Phys. Rev. Lett.* **62**, 1177 (1989).
 - [2] R. R. Gerhardts, D. Weiss, and K. v. Klitzing, *Phys. Rev. Lett.* **62**, 1173 (1989); C. W. J. Beenakker, *ibid* **62**, 2020 (1989); P. Vasilopoulos and F. M. Peeters, *ibid* **63**, 2120 (1989); P. Streda and A.H. MacDonald, *Phys. Rev. B* **41**, 11892 (1990); F. M. Peeters and P. Vasilopoulos, *ibid* **42**, R5899 (1990).
 - [3] F. M. Peeters and P. Vasilopoulos, *Phys. Rev. B* **46**, 4667(1992).
 - [4] S. Datta and B. Das, *Appl. Phys. Lett.* **56**, 665 (1990); X. F. Wang, P. Vasilopoulos, and F. M. Peeters, *Phys. Rev. B* **65**, 165217 (2002).
 - [5] D. D. Awschalom and J. M. Kikkawa, *Physics Today*, **52**, No. 6, 33 (1999).
 - [6] E. Tutuc, E. P. De Poortere, S. J. Papadakis, and M. Shayegan, *Phys. Rev. Lett.* **86**, 2858 (2001).
 - [7] J. P. Lu, J. B. Yau, S. P. Shukla, M. Shayegan, L. Wissinger, U. Rossler, and R. Winkler, *Phys. Rev. Lett.* **81**, 1282 (1998).
 - [8] A. G. Aronov and Y. B. Lyanda-Geller, *Phys. Rev. Lett.* **70**, 343 (1993); A. F. Morpurgo, J. P. Heida, T. M. Klapwijk, and B. J. van Wees, and G. Borghs, *ibid.* **80**, 1050 (1998); B. Molnar, F. M. Peeters, and P. Vasilopoulos, *Phys. Rev. B* **69**, 155335 (2004).
 - [9] S. D. Ganichev, E. L. Ivchenko, V. V. Bel'kov, S. A. Tarasenko, M. Sollinger, D. Weiss, W. Wegscheider, and W. Prettl, *Nature (London)* **417**, 153 (2002).
 - [10] F. Mireles and G. Kirczenow, *Phys. Rev. B* **66**, 214415 (2002).
 - [11] J. Sinova, D. Culcer, Q. Niu, N. A. Sinitsyn, T. Jungwirth, and A. H. MacDonald, *Phys. Rev. Lett.* **92**, 126603 (2004).
 - [12] G. Dresselhaus, *Phys. Rev.* **100**, 580 (1955); E. A. de Andrada e Silva, G. C. La Rocca, and F. Bassani, *Phys. Rev. B* **50**, 8523 (1994).
 - [13] E. I. Rashba, *Sov. Phys. Solid State* **2**, 1109 (1960).
 - [14] H. L. Stormer and Z. Schlesinger, A. Chang, D. C. Tsui, A. C. Gossard, and W. Wiegmann, *Phys. Rev. Lett.* **51**, 126 (1983).
 - [15] J. Luo, H. Munekata and F. F. Fang, P. J. Stiles, *Phys. Rev. B* **38**, R10142 (1988); B. Das,

- D. C. Miller, S. Datta, R. Reifenberger, W. P. Hong, P. K. Bhattacharya, J. Singh, and M. Jaffe, *ibid.* **39**, R1411 (1989).
- [16] Y. A. Bychkov and E. I. Rashba, *J. Phys. C* **17**, 6039 (1984).
- [17] X. F. Wang and P. Vasilopoulos, *Phys. Rev. B* **67**, 085313 (2003).
- [18] L. Magaril, *Superl. Microstruct.* **16**, 257 (1994).
- [19] J. Nitta, T. Akazaki, H. Takayanagi, T. Enoki, *Phys. Rev. Lett.* **78**, 1335 (1997).
- [20] G. Engels, J. Lange, Th. Schäpers, and H. Lüth, *Phys. Rev. B* **55**, R1958 (1997).
- [21] P. Vasilopoulos and C. M. Van Vliet, *J. Math. Phys.* **25**, 1391 (1984).
- [22] J. Shi, F. M. Peeters, K. W. Edmonds, and B. L. Gallagher, *Phys. Rev. B* **66**, 035328 (2002).
- [23] For *strong* 1D modulations oscillations in σ_{xy}^{nd} have been observed by K. W. Edmonds, B. L. Gallagher, P. C. Main, N. Overend, R. Wirtz, A. Nogaret, M. Henini, C. H. Marrows, B. J. Hickey, and S. Thoms, *Phys. Rev. B* **64**, 041303(R) (2001).